AMERICAN SOCIETY FOR MICROBIOLOGY | Molecular and Cellular Biology

The Mediator Subunit MED16 Transduces NRF2-Activating Signals into Antioxidant Gene Expression

Hiroki Sekine,[a,b] Keito Okazaki,[b] Nao Ota,[b] Hiroki Shima,[c,d] Yasutake Katoh,[e] Norio Suzuki,[f] Kazuhiko Igarashi,[c] Mitsuhiro Ito,[g] Hozumi Motohashi,[b] Masayuki Yamamoto[a,e]

Department of Medical Biochemistry,[a] Department of Biochemistry,[c] and Division of Interdisciplinary Medical Science,[f] Tohoku University Graduate School of Medicine, Sendai, Japan; Department of Gene Expression Regulation, Institute of Development, Aging and Cancer, Tohoku University, Sendai, Japan[b]; CREST, AMED, Sendai, Japan[d]; Tohoku Medical Megabank Organization, Tohoku University, Sendai, Japan[e]; Laboratory of Hematology, Division of Medical Biophysics, Kobe University Graduate School of Health Sciences, Kobe, Japan[g]

The KEAP1-NRF2 system plays a central role in cytoprotection. NRF2 is stabilized in response to electrophiles and activates transcription of antioxidant genes. Although robust induction of NRF2 target genes confers resistance to oxidative insults, how NRF2 triggers transcriptional activation after binding to DNA has not been elucidated. To decipher the molecular mechanisms underlying NRF2-dependent transcriptional activation, we purified the NRF2 nuclear protein complex and identified the Mediator subunits as NRF2 cofactors. Among them, MED16 directly associated with NRF2. Disruption of *Med16* significantly attenuated the electrophile-induced expression of NRF2 target genes but did not affect hypoxia-induced gene expression, suggesting a specific requirement for MED16 in NRF2-dependent transcription. Importantly, we found that 75% of NRF2-activated genes exhibited blunted inductions by electrophiles in *Med16*-deficient cells compared to wild-type cells, which strongly argues that MED16 is a major contributor supporting NRF2-dependent transcriptional activation. NRF2-dependent phosphorylation of the RNA polymerase II C-terminal domain was absent in *Med16*-deficient cells, suggesting that MED16 serves as a conduit to transmit NRF2-activating signals to RNA polymerase II. MED16 indeed turned out to be essential for cytoprotection against oxidative insults. Thus, the KEAP1-NRF2-MED16 axis has emerged as a new regulatory pathway mediating the antioxidant response through the robust activation of NRF2 target genes.

The KEAP1 (Kelch-like ECH-associated protein 1)-NRF2 (nuclear factor erythroid 2-related factor 2) system is the major regulatory pathway for cytoprotection from oxidative insults (1, 2). NRF2 is a potent transcriptional activator that coordinately regulates cytoprotective genes whose products are involved in glutathione synthesis, elimination of reactive oxygen species (ROS), and detoxification of xenobiotics. Under unstressed conditions, NRF2 is trapped by KEAP1, ubiquitinated, and degraded by proteasomes. KEAP1 is inactivated upon exposure to electrophilic chemicals, resulting in the stabilization of NRF2 and the activation of NRF2 target genes. NRF2 heterodimerizes with small Maf proteins (sMAF) and binds to the antioxidant response element (ARE) [(A/G)TGA(G/C)NNNGC], which is commonly found in the regulatory regions of the cytoprotective genes activated by NRF2. Recent analyses of the genome-wide distribution of NRF2 characterized the set of *cis*-acting targets of NRF2 on a genome-wide scale (the NRF2 cistrome), in which the ARE sequence has been selected as the most highly enriched motif (3–5).

Mediator is an evolutionarily conserved multiprotein complex consisting of approximately 30 subunits and is required for transcription driven by RNA polymerase II (RNAP II) (6, 7). Mediator plays a canonical role in connecting DNA-binding transcription factors with the basal transcription machinery containing RNAP II. Biochemical and structural approaches have revealed four modules in the Mediator complex: the head, middle, tail, and kinase modules. The head and middle modules are involved in the association with the basal transcription machinery, whereas the tail module is targeted by various signal-specific transcription factors (6). For instance, sterol regulatory element binding protein (SREBP) responding to lipid metabolism status and ELK responding to mitogen-activated protein kinase (MAPK) signaling directly interact with MED15 and MED23, respectively, in the tail module. Therefore, Mediator functions as a "hub," receiving and integrating various regulatory signals for the inducible transcription of signal-specific genes. Currently, a Mediator subunit that receives electrophilic stress signals has not been identified.

Six Neh (NRF2-ECH homology) domains have been defined in NRF2 based on species conservation (8). The Neh1 domain contains the basic region-leucine zipper motif, mediating DNA binding and dimerization. The Neh2 and Neh6 domains contain degrons responsible for KEAP1-CUL3-dependent and βTrCP (beta-transducin repeat-containing E3 ubiquitin protein ligase)-CUL1-dependent degradation, respectively (9, 10). The other domains, namely, Neh4, Neh5, and Neh3, are considered transactivation domains. CREB binding protein (CBP) and BRG1 (SMARCA4) associate with the Neh4 and Neh5 domains (11, 12), and chromodomain helicase DNA binding protein 6 (CHD6) associates with the Neh3 domain (13). However, the functional sig-

Received 9 August 2015 **Returned for modification** 2 September 2015
Accepted 10 November 2015

Accepted manuscript posted online 16 November 2015

Citation Sekine H, Okazaki K, Ota N, Shima H, Katoh Y, Suzuki N, Igarashi K, Ito M, Motohashi H, Yamamoto M. 2016. The Mediator subunit MED16 transduces NRF2-activating signals into antioxidant gene expression. Mol Cell Biol 36:407–420. doi:10.1128/MCB.00785-15.

Address correspondence to Hozumi Motohashi, hozumim@med.tohoku.ac.jp, or Masayuki Yamamoto, masiyamamoto@med.tohoku.ac.jp.

Supplemental material for this article may be found at http://dx.doi.org/10.1128/MCB.00785-15.

nificance of the interaction with these factors for NRF2-mediated cytoprotection against oxidative insults has not been evaluated. Moreover, a general understanding of how NRF2 conveys the activation signal to the basal transcription machinery and triggers the robust induction of its target genes after binding to the ARE has not been established.

To identify an essential transcription cofactor of NRF2 for the antioxidant response, we purified and characterized the NRF2 nuclear protein complex. We identified several Mediator subunits as novel NRF2-associating proteins. Of these, MED16 directly interacted with NRF2 and was essential for the inducible expression of the majority of the NRF2 target genes. Importantly, MED16 deficiency remarkably sensitized cells to oxidative insults. Thus, this study has clarified a missing piece between NRF2 and the basal transcription machinery and revealed the critical contribution of the KEAP1-NRF2-MED16 axis to the defense mechanism against oxidative insults.

MATERIALS AND METHODS

Cell culture. 293F, Hepa1c1c7, and Hep3B cells were maintained in low-glucose Dulbecco's modified Eagle's medium (DMEM) (Wako) supplemented with 10% fetal bovine serum (Sigma) and penicillin-streptomycin (Gibco) under 5.0% CO_2 at 37°C.

Mice. *Pten*$^{flox/flox}$ and *Keap1*$^{flox/flox}$ mice were described previously (14, 15). The *Pten*$^{flox/+}$ line of mice was a kind gift from Akira Suzuki (Kyushu University). *Albumin*-Cre transgenic mice were purchased from The Jackson Laboratory (Bar Harbor, ME) (16). *Pten*$^{flox/flox}$::*Keap1*$^{flox/flox}$::*Albumin*-Cre mice (PK-Alb mice) were obtained from matings between *Pten*$^{flox/flox}$::*Keap1*$^{flox/flox}$ and *Pten*$^{flox/flox}$::*Keap1*$^{flox/+}$::*Albumin*-Cre mice and were sacrificed for liver protein preparation. The mice were provided water and rodent chow *ad libitum*. All mice were maintained under specific-pathogen-free conditions and treated according to the regulations of the standards for human care and use of laboratory animals of Tohoku University and the guidelines for proper conduct of animal experiments of the Ministry of Education, Culture, Sports, Science, and Technology of Japan. All the animal experiments were approved by The Tohoku University Committee for Laboratory Animal Research.

Chemicals. Diethyl maleate (DEM) and dimethyl sulfoxide (DMSO) were purchased from Wako Pure Chemicals. Menadione was purchased from Sigma-Aldrich. Dithiobis succinimidyl propionate (DSP) was purchased from Pierce.

Plasmids. pQC-FLAG-hNRF2 T80R and FLAG-hMED10 were generated by inserting FLAG-hNRF2 T80R and FLAG-hMED10 cDNA fragments, respectively, into the pQCXIP vector (Clontech). pGEX4T-1 mNRF2 mutant vectors were generated by inserting cDNAs encoding various mNRF2 truncations into pGEX4T-1. pcDNA3-FLAG-hMED24, pcDNA3-FLAG-hMED23, pcDNA3-FLAG-hMED16, and pcDNA3-FLAG-hMED14 were generated by inserting hMED24, hMED23, hMED16, and hMED14 cDNAs, respectively, into the pcDNA3FLAG vector. pcDNA3-FLAG-hMED16-A, -B, -C, and -D were generated by inserting truncated hMED16 cDNAs (encoding amino acids 2 to 212, 213 to 434, 435 to 650, and 651 to 877, respectively) into the pcDNA-3FLAG vector. The pX330-mMED16 gRNA vector was created by inserting an annealed oligonucleotide pair (5′-CACCGGCCATCACCTGCCTGGAG T-3′ and 5′-AAACACTCCAGGCAGGTGATGGCC-3′) into the BpiI sites of pX330.

Generation of stable transformant cell lines. To obtain retroviruses for the establishment of FLAG-hNRF2 T80R-expressing cells, FLAG-hMED10-expressing cells, and cells harboring a vacant vector, the pQC-FLAG-hNRF2 T80R, pQC-FLAG-hMED10, and pQCXIP vectors, respectively, were transfected into PLAT-A cells. The medium was changed after 24 h of transfection, and the cells were cultured in fresh medium for an additional 24 h. The retrovirus particles were produced in the medium, which was used for the transduction of 293F cells (Life Technologies), Hepa1c1c7 cells, and *Med16*-deficient Hepa1c1c7 cells (*Med16* KO 1 cells [see below]). These cells were transduced with the respective retroviruses in a suspension with 12 μg/ml of Polybrene. One day after infection, infected cells were replated and incubated in a selection medium containing 2 μg/ml of puromycin (Sigma). For the establishment of stable cell lines expressing FLAG-hMED24, FLAG-hMED23, FLAG-hMED16, and FLAG-hMED14, 293F cells were transfected with pcDNA3-FLAG-hMED24, pcDNA3-FLAG-hMED23, pcDNA3-FLAG-hMED16, and pcDNA3-FLAG-hMED14, respectively. After transfection, the cells were replated and incubated with selection medium containing 1.5 mg/ml Geneticin (Nacalai Tesque).

Identification of NRF2-interacting proteins in 293F cells. A nuclear extract was prepared from FLAG-hNRF2 T80R-expressing 293F cells. The nuclear extract was subjected to anti-FLAG affinity purification. The FLAG-hNRF2 T80R complex was eluted by using the FLAG peptide according to the manufacturer's protocol (Sigma). The eluate was subjected to nanoscale high-performance liquid chromatography–tandem mass spectrometry (nanoLC-MS/MS) analysis, and NRF2-associated proteins were identified through protein sequence database searching.

NanoLC-MS/MS analysis and protein sequence database searches. Trypsin-digested peptides were dissolved in sample solution (5% acetonitrile and 0.1% trifluoroacetic acid [TFA]). Each sample was injected into an EasynLC-1000 system (Thermo Scientific) connected to an EASY-Spray column (C_{18} column of 25-cm length by 75-μm diameter; Thermo Scientific). Peptides were eluted with a 120-min gradient of 4% to 35% solvent B (0.1% formic acid in acetonitrile [vol/vol]) in solvent A (0.1% formic acid in water [vol/vol]) at a flow rate of 300 nl/min. Peptides were then ionized and analyzed by use of a Q-Exactive mass spectrometer (Thermo Scientific) using a nano-spray source. High-resolution full-scan MS spectra (from *m/z* 380 to 1,800) were acquired with an Orbitrap device with a resolution (R) of 70,000 at *m/z* 400 and lock mass enabled (*m/z* 445.12003 and 391.28429), followed by MS/MS fragmentation of the 10 most intense ions in the linear ion trap with a high collisionally activated dissociation (HCD) energy of 35%. The exclusion duration for the data-dependent scan was 0 s, and the isolation window was set at *m/z* 2.0.

The MS/MS data were analyzed by sequence alignment using variable and static modifications with Mascot algorithms. The protein database utilized was Swiss-Plot, which considers each peptide sequence in trypsin-digested fragment patterns. The specific parameters for protein sequence database searching included oxidation (M), deamination (N and Q), acetylation (N-terminal), and pyroglutamation (E) as variable modifications and carbamidomethylation (C) as a static modification. Other parameters used in data analysis were as follows: two allowed missing cleavages and mass errors of 10 ppm for precursor ions and 0.02 Da for fragment ions. Charge states of +2 to +4 were considered for parent ions. If more than one spectrum was assigned to a peptide, only the spectrum with the highest Mascot score was selected for manual analysis.

Generation of *Nrf2* knockdown cell lines. Lentiviral particles expressing control short hairpin RNA (shRNA) and mNrf2 shRNAs (TRCN54659 and TRCN54658) were purchased from Sigma-Aldrich. Hepa1c1c7 cells were infected for 24 h with lentivirus at a multiplicity of infection of 10. Infected cells were washed with phosphate-buffered saline (PBS), followed by 12 h of incubation. The cells were replated and incubated in a selection medium containing 2 μg/ml of puromycin (Sigma).

Generation of *Med16* knockout cell lines. Hepa1c1c7 cells (1.5×10^5 cells/well) were plated in 6-well plates 24 h prior to transfection. Cells were cotransfected with 2 μg pX330-mMED16 gRNA and 0.2 μg pcDNA3 by use of Lipofectamine 2000 (Life Technologies). pcDNA3 was included to confer Geneticin resistance as a selection marker. The medium was changed after 24 h of transfection. After another 24 h of incubation, the cells were replated in 10-cm dishes and incubated with selection medium containing 1.5 mg/ml Geneticin (Nacalai Tesque). Among the Geneticin-resistant healthy clones, two clones, *Med16* KO 1 and *Med16* KO 2, were arbitrarily selected and used for further analyses. Disruption of the *Med16* gene was verified by sequencing the DNA surrounding the target site of

the guide RNA (gRNA). Genomic DNAs were purified from the two clones and used as templates for PCR amplification of the DNA fragment spanning the gRNA target site by using the following primer set: mMed16 CRISPR seq F (5′-CAG CAT CAG CAG ACA GTA GCC G-3′) and mMed16 CRISPR seq R (5′-GTG GGG ACA CAG GCA CTT CG-3′). The amplified DNA fragments were inserted into the EcoRV site of pcDNA3 and used for bacterial transformation. Nine and 10 bacterial colonies were picked up for *Med16* KO 1 and 2, respectively, and purified plasmids were sequenced using the T7 primer (5′-TAA TAC GAC TCA CTA TAG GG-3′) and the pcDNA3 3′ primer (5′-TAG AAG GCA CAG TCG AGG-3′).

Microarray analysis and definition of NRF2-activated genes. Hepa1c1c7 cells with *Nrf2* shRNA (*Nrf2* KD cells; samples 1 and 2), Hepa1c1c7 cells with control shRNA (sh-control cells; samples 3 and 4), *Med16* KO Hepa1c1c7 cells (*Med16* KO cells; samples 5 and 6), and parent Hepa1c1c7 cells (wild-type [WT] cells; samples 7 and 8) were cultured and harvested after 12 h of treatment with 100 μM DEM (samples 1, 3, 5, and 7) or with DMSO (vehicle) (samples 2, 4, 6, and 8), and total RNAs were purified. The total RNAs were processed and hybridized to a 4 × 44K whole-mouse-genome microarray (Agilent Technologies). GeneChip experiments were performed according to the manufacturer's protocol. The arrays were scanned using a G2539A microarray scanner system (Agilent Technologies).

The resulting data were analyzed using GeneSpring GX software (Agilent Technologies). NRF2-activated genes were defined as follows. Genes were selected as DEM-activated genes if they satisfied both of the following conditions: $\log_2$ (sample 3/sample 4) · $\log_2$ fold change for sh-control cells of >0.5 and $\log_2$ (sample 7/sample 8) · $\log_2$ fold change for WT cells of >0.5. Among the DEM-activated genes, NRF2-dependent DEM-activated genes (NRF2-activated genes) were selected if they satisfied the following condition: $\log_2$ (sample 1/sample 2) · $\log_2$ fold change for *Nrf2* KD cells < $\log_2$ (sample 3/sample 4) · $\log_2$ fold change for sh-control cells. Consequently, 848 genes were defined as NRF2-activated genes. Values for $\log_2$ (sample 5/sample 6) · $\log_2$ fold change for *Med16* KO cells and $\log_2$ (sample 7/sample 8) · $\log_2$ fold change for WT cells for the 848 genes were arranged in a heat map, in which the 848 genes were aligned in declining order of values for $\log_2$ (sample 7/sample 8) · $\log_2$ fold change for WT cells − $\log_2$ (sample 5/sample 6) · $\log_2$ fold change for *Med16* KO cells.

Immunoblot analysis. Immunoblot analysis was performed as described previously (17). The antibodies used were as follows: anti-FLAG (F7425; Sigma), anti-MED24 (A301-472A; Bethyl Laboratories), anti-MED23 (ab70450; Abcam), anti-MED16 (ab130996; Abcam), anti-MED1 (sc-8998; Santa Cruz), anti-MED7 (ab50687; Abcam), anti-hNRF2 (sc-13032; Santa Cruz), antitubulin (T9026; Sigma), and anti-mNRF2 (18) antibodies.

Protein preparations from cell lines. Glutathione *S*-transferase (GST) fusion proteins of various NRF2 mutants were expressed in *Escherichia coli* strain BL21(DE3), and soluble lysates were prepared in PBS-T (PBS with 0.1% Tween 20) by sonication. For Mediator complex purification, soluble nuclear extracts were prepared from 293F cells, Hepa1c1c7 cells, and *Med16* KO Hepa1c1c7 cells stably expressing FLAG-hMED10 (19). The nuclear extracts were subjected to anti-FLAG affinity purification. FLAG-Mediator complexes were eluted by using the FLAG peptide according to the manufacturer's protocol (Sigma). Recombinant FLAG-hMED24, FLAG-hMED23, FLAG-hMED16, and FLAG-hMED14 were expressed in 293F cells and purified by the same procedure as that for Mediator complex purification. To prepare whole-cell extracts containing FLAG-hMED16-A, -B, -C, and -D, 293T cells were transiently transfected with pcDNA3-FLAG-hMED16-A, -B, -C, and -D, respectively. The transfected cells were lysed with radioimmunoprecipitation assay (RIPA) buffer, and supernatants were obtained in the same manner as that for the whole-cell extracts. For NRF2 detection, cells were harvested after 4 h of treatment with 100 μM DEM or DMSO (vehicle), and nuclear extracts were prepared.

GST pulldown assay. Glutathione-Sepharose-immobilized GST and GST-mNRF2 mutants were incubated with nuclear or whole-cell extracts, recombinant Mediator subunits, or purified Mediator complexes and washed extensively with PBS-T. The GST pulldown/cross-linking assay was performed as described previously (20). GST-Neh4/5 (85–210), namely, a construct with the Neh4 and Neh5 domains of NRF2 (amino acids 85 to 210) linked with GST, was incubated with the purified Mediator complex and washed extensively with PBS-T (PBS with 0.1% Tween 20). Subsequently, beads were equilibrated and resuspended in buffer (20 mM HEPES [pH 7.9] and 100 mM KCl), followed by incubation with various concentrations of DSP (Pierce) to introduce reversible cross-links between directly interacting proteins. After incubation for 10 min at room temperature, the cross-linking reaction was quenched by addition of 2 M Tris-HCl (pH 7.5) and subsequently terminated by addition of quenching buffer (30 mM Tris-HCl [pH 7.5] and 100 mM NaCl) for 15 min at room temperature. Un-cross-linked proteins were removed with urea wash buffer (30 mM Tris-HCl [pH 7.5], 100 mM KCl, and 8 M urea). Proteins retained on beads were eluted in Laemmli sample buffer at 94°C. Eluates were resolved by 10% SDS-PAGE and analyzed by immunoblot assay for the presence of Mediator subunits.

RNA purification and quantitative RT-PCR. Total RNA samples were prepared from cells treated with 100 μM DEM or DMSO (vehicle) for 12 h and those exposed to 1% O_2 (hypoxia) or 20% O_2 (normoxia) for 24 h by using Sepasol RNA I Super G solution (Nacalai Tesque). The cDNAs were synthesized from 0.5 μg of total RNA by using ReverTra Ace qPCR reverse transcription (RT) master mix with gDNA Remover (Toyobo). Real-time PCR was performed in triplicate for each sample, using a StepOnePlus real-time PCR system (Applied Biosystems) and the primers listed in Table 1. Expression levels of hypoxanthine phosphoribosyltransferase (HPRT) were used as internal controls for normalization.

siRNA transfection. Hep3B cells were transfected with 20 to 50 nM small interfering RNA (siRNA) against MED16 by using RNAiMAX (Invitrogen) according to the manufacturer's protocol. After 48 h of transfection, cells were treated with 100 μM DEM or exposed to 1% O_2. siRNA was ordered through a predesigned siRNA library (Qiagen).

Identification of NRF2-interacting proteins in mouse liver. For detection of endogenous interactions between NRF2 and the Mediator complex, *Pten*$^{flox/flox}$::*Keap1*$^{flox/flox}$::*Albumin*-Cre mouse livers were homogenized in 0.1× PBS containing 0.5 mM dithiobismaleimidoethane (DTME) (Thermo Scientific) and 0.5 mM DSP (Thermo Scientific) and incubated at 4°C for 2 h, followed by incubation in quenching buffer (20 mM Tris-HCl [pH 7.5], 5 mM cysteine) at 4°C for 20 min. After washing with PBS, the sample was resuspended in lysis buffer (20 mM HEPES [pH 7.6], 20% glycerol, 10 mM NaCl, 1.5 mM $MgCl_2$, 0.2 mM EDTA) and put on ice for 10 min. After centrifugation at 600 × *g* at 4°C for 10 min, the pellet was briefly sonicated in RIPA buffer and then centrifuged at 10,000 × *g* at 4°C for 10 min. The supernatant was subjected to anti-NRF2 affinity purification. Anti-NRF2 antibody (D1Z9C-XP; Cell Signaling Technology) was cross-linked to Dynabeads anti-rabbit IgG (Thermo Scientific) with dimethyl pimelimidate dihydrochloride (Sigma-Aldrich). The NRF2 complex was eluted from the beads by incubation at 37°C for 20 min in elution buffer (50 mM Tris-HCl [pH 8.0], 0.2 M NaCl, 2% SDS, 50 mM dithiothreitol [DTT]). The eluate was subjected to gel-based LC-MS/MS analysis.

Gel-based LC-MS/MS analysis and protein sequence database searches. The detailed protocol for the gel-based LC-MS/MS analysis will be published elsewhere (37; H. Tanaka, A. Muto, K. Ochiai, H. Shima, Y. Katoh, N. Sax, S. Tajima, A. Brydun, T. Ikura, N. Yoshizawa, H. Masai, Y. Hosikawa, T. Noda, M. Nio, and K. Igarashi, submitted for publication). After SDS-PAGE using a 5 to 20% polyacrylamide gradient gel (Oriental Instruments) and Coomassie brilliant blue (CBB) staining (21), each lane in the gel was divided into 17 sections. The resulting gel blocks were treated with DTT and acrylamide for reduction and alkylation of the sulfhydryl groups. After overnight tryptic digestion, the resulting peptides in each gel block were extracted, and one half of each sample was subjected to LC-MS/MS using an LTQ Orbitrap Velos mass spectrometer (Thermo

TABLE 1 Primers and probes used for mouse (m) and human (h) mRNA expression

Primer or probe	Sequence (5′–3′)[a]
mNqo1 forward	AGCTGGAAGCTGCAGACCTG
mNqo1 reverse	CCTTTCAGAATGGCTGGCA
mNqo1 probe	FAM-ATTTCAGTTCCCATTGCAGTGGTTTGGG-TAMRA
mGpx2 forward	TGTCAGAACGAGGAGATCCTG
mGpx2 reverse	GACTAAAGGTGGGCTGGTACC
mGclm forward	TGACTCACAATGACCCGAAA
mGclm reverse	GATGCTTTCTTGAAGAGCTTCCT
mGclc forward	ATCTGCAAAGGCGGCAAC
mGclc reverse	ACTCCTCTGCAGCTGGCTC
mGclc probe	FAM-ACGGGTGCAGCAAGGCCCA-TAMRA
mGlut1 forward	CCATGGATCCCAGCAGCAAG
mGlut1 reverse	CCAGTGTTATAGCCGAACTGC
mBnip3 forward	GTTACCCACGAACCCCACTTT
mBnip3 reverse	GTGGACAGCAAGGCGAGAAT
mPgk1 forward	GATGCTTTCCGAGCCTCACTGT
mPgk1 reverse	ACCAGCCTTCTGTGGCAGATTC
mVegfa forward	CTGCTGTAACGATGAAGCCCTG
mVegfa reverse	GCTGTAGGAAGCTCATCTCTCC
m18SrRNA forward	CGGCTACCACATCCAAGGAA
m18SrRNA reverse	GCTGGAATTACCGCGGCT
m18SrRNA probe	FAM-TGCTGGCACCAGACTTGCCCTC-TAMRA
hNqo1 forward	GTCATTCTCTGGCCAATTCAGAGT
hNqo1 reverse	TTCCAGGATTTGAATTCGGG
hNqo1 probe	FAM-ACTGACATATAGCATTGGGCACACTCCAG-TAMRA
hGCLM forward	TAGAATCAAACTCTTCATCATCAACTAGA
hGCLM reverse	TCACAGAATCCAGCTGTGCAA
hGCLM probe	FAM-TGCAGTTGACATGGCCTGTTCAGTCC-TAMRA
hGCLC forward	TCTCTAATAAAGAGATGAGCAACATGC
hGCLC reverse	TTGACGATAGATAAAGAGATCTACGAA
hGCLC probe	FAM-CAGGAGATGATCAATGCCTTCCTGCAAC-TAMRA
hCA9 forward	CCTTTGCCAGAGTTGACGAG
hCA9 reverse	GACAGCAACTGCTCATAGGC
hBNIP3 forward	CCAAGAGCTCTCACTGTGAC
hBNIP3 reverse	GCTCTGTTGGTATCTTGTGG
hPGK1 forward	CTAACAAGCTGACGCTGGAC
hPGK1 reverse	CTGGTTGTTTGTTATCTGGTTG
hNRF2 forward	TCATGATGGACTTGGAGCTG
hNRF2 reverse	CATACTCTTTCCGTCGCTGA
hHPRT forward	CCGGCTCCGTTATGGC
hHPRT reverse	GGTCATAACCTGGTTCATCATCA
hHPRT probe	FAM-CGCAGCCCTGGCGTCGTGATTA-TAMRA

[a] FAM, 6-carboxyfluorescein; TAMRA, 6-carboxytetramethylrhodamine.

Scientific). The data acquisition for every sample was done for 60 min after a 50-min LC gradient was started, where MS^1 scans from *m/z* 321 to 1,600 were carried out in the Orbitrap device, with the resolution set at 60,000 and a lock mass at *m/z* 445.120025, followed by top-15 MS^2 acquisition by collision-induced dissociation (CID) in the ion trap in the normal resolution mode. The settings for the MS^2 scans were as follows: minimal signal intensity required = 500, AGC target = 5,000, and maximum ion injection time = 50 ms (22). The raw data files derived from samples in the same SDS-PAGE gel lane were converted together into a single MASCOT generic format file and used for database searches by MASCOT (version 2.5.1; Matrix Science) against the mouse proteins in Swiss-Prot (August 2015) and a custom database including contaminant proteins. The peptide expectation value cutoff was set at 0.05. Protein N-terminal acetylation (+42.0106), oxidation of methionine (+15.9949), propionamidated cysteine (+71.0371), propionamidated DSP (at lysine) (+159.0354), and propionamidated DTME (at cysteine) (+246.0674) were considered possible variable modifications. The false-discovery rates (FDR) were automatically adjusted to 1% by MASCOT Percolator for every search.

ChIP assay. Chromatin immunoprecipitation (ChIP) assays were performed with WT and *Med16* KO Hepa1c1c7 cells by using anti-NRF2 (D1Z9C-XP; Cell Signaling Technology), anti-CBP (sc-369X; Santa Cruz), and anti-RNAP II C-terminal domain (CTD), anti-RNAP II pSer5, and anti-RNAP II pSer2 (kind gifts from H. Kimura) (23) antibodies. For samples incubated with anti-NRF2, anti-RNAP II pSer5, and anti-RNAP II pSer2 antibodies, the cells were treated with 100 μM DEM or DMSO (vehicle) for 4 h, fixed with 1% formaldehyde for 10 min, lysed, and sonicated for DNA shearing. For samples incubated with anti-CBP and anti-RNAP II CTD antibodies, the cells were treated with 100 μM DEM or DMSO (vehicle) for 4 h, cross-linked with 1.5 mM ethylene glycol bis(succinimidyl succinate) (EGS) (Thermo Scientific) for 20 min followed by 1% formaldehyde for 10 min, lysed, and digested with micrococcal nuclease (New England BioLabs) for DNA shearing. The nuclear lysis solution was incubated overnight with a specific antibody, followed by incubation with an equal mixture of Dynabeads protein A and protein G (Life Technologies) bound by a respective secondary antibody. Precipitated DNA was analyzed by real-time PCR using the primer sets described in Table 2. ChIP assays were also performed with A549 cells with or without

TABLE 2 Primers used for ChIP assays

Primer	Sequence (5′–3′)
mNqo1 ARE forward	GCACGAATTCATTTCACACGAGG
mNqo1 ARE reverse	GCTCAAATTTTGCCGACTCACTG
mNqo1 pro forward	AGCCAATCAGCGTTCGGTAT
mNqo1 pro reverse	AACTCACAGCCAGCCCCTAC
mNqo1 ex6 forward	AGTGGCATCCTGCGTTTCT
mNqo1 ex6 reverse	TCTCCTCCCAGACGGTTTCC
mGclm ARE forward	CGAGACAAAAGAGCAGACTC
mGclm ARE reverse	GTAATCTACATTTCCTTTGGCTG
mGclm pro forward	ACGGTTACGAAGCACTTTCT
mGclm pro reverse	AACGAGGGAGCTGTTTCCTG
mGclm ex7 forward	TGAAGAGCAGGGGAATCATC
mGclm ex7 reverse	GACAACAGCAGGTCGGTGAG
mGclc ARE forward	TGCTGAGTCACGGTGAGGCG
mGclc ARE reverse	CCGTTGTTGTGGTAGCGCCG
mGclc pro forward	CACTGAGCTGGGAAGAGACC
mGclc pro reverse	TGTGCAGGAACTGGAGGATG
mGclc ex16 forward	CGCTCTTCCATTACCACCTG
mGclc ex16 reverse	AGCCTGTCAATCTGCTCCTG
hNQO1 ARE forward	CATGTCTCCCCAGGACTCTC
hNQO1 ARE reverse	TTTTAGCCTTGGCACGAAAT
hGCLM ARE forward	GGAGAGCTGATTCCAAACTG
hGCLM ARE reverse	GAGTAACGGTTACGAAGCAC
hNQO1exon2 forward	CGTGTGTGCTTTGTGTGTGT
hNQO1 exon2 reverse	GCCTCCTTCATGGCATAGTT

NRF2 knockdown by using anti-NRF2 (D1Z9C-XP; Cell Signaling Technology) and anti-MED16 (ab130996; Abcam) antibodies. Control siRNA (87109120 DS scrambled negative control; Invitrogen) or NRF2 siRNA (HSS107128; Invitrogen) was electroporated into A549 cells by use of an MP-100 MicroPorator (Digital Bio Technology). Cells were harvested for the ChIP assay after 36 h of electroporation. Cross-linking was performed using 1.5 mM EGS and 1% formaldehyde in the same way as that described above, and micrococcal nuclease was used for DNA shearing.

Cell viability study. Cell viability after menadione (Sigma-Aldrich) treatment was determined using a Cell Counting kit 8 (Nacalai Tesque) according to the manufacturer's protocol.

RESULTS

Identification of Mediator subunits as interacting proteins of NRF2. To clarify a mechanism of transcriptional activation in response to electrophilic/oxidative stresses, we analyzed a nuclear protein complex containing NRF2. To obtain unbiased binding partner proteins of NRF2 in the nucleus, we established a 293F cell line stably expressing FLAG-tagged NRF2-T80R, which is a constitutively active NRF2 mutant that escapes KEAP1-dependent degradation (24). The FLAG-NRF2-T80R-containing protein complex was biochemically purified using the anti-FLAG antibody. The purified proteins were subjected to nanoLC-MS/MS analysis. We identified CBP and p300 (Fig. 1A), which are known transcriptional coactivators of NRF2 (11). The NRF2 protein complex also contained MED24, MED23, MED16, and MED14, which are components of the tail module of the Mediator complex (Fig. 1A). MED24, MED23, and MED16 closely associate with one another, forming a submodule (25, 26).

The large size and shape of the Mediator complex provide an extensive surface area facilitating multiple protein-protein interactions, which enables Mediator to serve as a scaffold for various transcription factors regulating tissue-specific and/or stimulus-specific gene expression (6, 7). Expecting that a specific Mediator subunit participates as a key molecule in the NRF2-dependent antioxidant response, we focused on the analysis of the Mediator subunits.

To confirm the interaction between NRF2 and the Mediator complex, we performed immunoblot analysis of the NRF2 complex purified from FLAG-NRF2-T80R-expressing cells by using antibodies against the Mediator subunits (Fig. 1B). In addition to the tail module components MED16, MED23, and MED24, MED1 and MED7, which comprise the middle module, were also detected in the NRF2 complex, indicating that the Mediator subunits associating with NRF2 are not limited to those of the tail module.

The Mediator complex interacts with NRF2 via the Neh4/Neh5 and Neh1 domains. To identify the specific NRF2 domains required for the interaction with the Mediator complex, a series of GST-NRF2 fusion proteins were newly generated (Fig. 1C). The Mediator complex was purified from FLAG-MED10-expressing 293F cells as described previously (19). The GST-NRF2 mutant proteins were incubated with the Mediator complex, and MED23 and MED16 were detected as representative subunits after GST pulldown. MED23 and MED16 were pulled down with GST-NRF2 mutants 2 (GST-Neh2/4/5/6), 4 (GST-Neh4/5), 6 (GST-Neh6/1/3), and 8 (GST-Neh1) (Fig. 1D), suggesting that either the Neh4/Neh5 domains or the Neh1 domain is sufficient for the association with the Mediator complex.

MED16 interacts directly with NRF2. To determine which Mediator subunits directly associate with NRF2, we prepared recombinant FLAG-tagged MED24, MED23, MED16, and MED14,

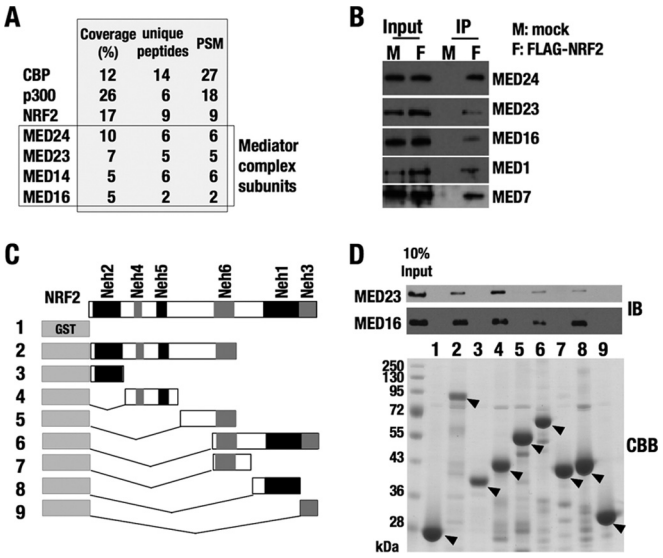

FIG 1 NRF2 associates with Mediator subunits. (A) NRF2-interacting proteins identified by LC-MS/MS. PSM, total peptide spectrum matches. (B) Immunoblot analysis of Mediator subunits in the FLAG-NRF2 nuclear complex. (C) GST fusion proteins with NRF2 mutants. 1, GST; 2, GST-Neh2/4/5/6 (1–407); 3, GST-Neh2 (1–84); 4, GST-Neh4/5 (85–210); 5, GST-Neh6u (211–407); 6, GST-Neh6/1/3 (319–598); 7, GST-Neh6d (319–408); 8, GST-Neh1 (408–554); 9, GST-Neh3 (555–598). (D) GST-NRF2 pulldown assay with the Mediator complex. The Mediator complex was purified from FLAG-MED10-expressing 293F cells by use of an anti-FLAG antibody and was incubated with GST-NRF2 mutants. MED23 and MED16 were detected as representatives of the Mediator subunits (upper panel), and protein staining of GST-NRF2 mutants is shown (lower panel). Arrowheads indicate the GST fusion proteins. CBB, Coomassie brilliant blue; IB, immunoblot.

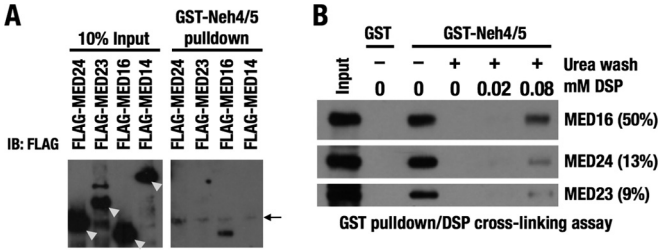

FIG 2 MED16 interacts directly with NRF2. (A) GST-NRF2 pulldown assay with FLAG-tagged recombinant MED24, MED23, MED16, and MED14. Arrowheads indicate the FLAG-tagged Mediator subunits. The arrow indicates nonspecific bands. (B) GST-NRF2 pulldown assay with the Mediator complex after DSP cross-linking. The Mediator complex was purified from FLAG-MED10-expressing 293F cells by use of an anti-FLAG antibody. Ratios of pulldown fractions after washing with urea are indicated in parentheses. GST-Neh4/5 was used for the pulldown.

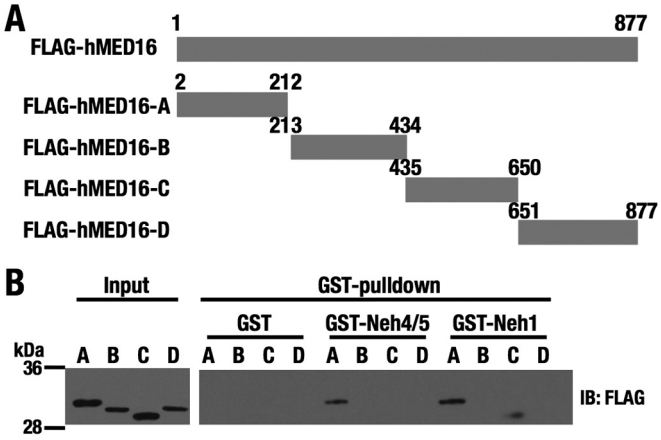

FIG 3 The N-terminal region of MED16 contains a major NRF2-interacting domain. (A) Dissection of MED16 into four parts. The full-length MED16 protein was divided into four fragments: A, B, C, and D. Each of the MED16 fragments was linked to the FLAG tag and overexpressed in 293T cells. (B) GST-NRF2 pulldown assay with whole-cell extracts expressing FLAG-tagged MED16-A, -B, -C, and -D. GST-Neh4/5 and GST-Neh1 were used for the pulldown assays.

which were identified in the NRF2 protein complex through LC-MS/MS. These recombinant proteins were incubated with GST-Neh4/5, and the pulldown samples were analyzed by immunoblot analysis with the anti-FLAG antibody. Recombinant MED16 interacted efficiently with GST-Neh4/5, but MED24, MED23, and MED14 did not (Fig. 2A).

To further verify the direct interaction between NRF2 and MED16, we conducted a GST pulldown/cross-linking assay (20). The Mediator complex purified from FLAG-MED10-expressing 293F cells was incubated with GST or GST-Neh4/5 and treated with increasing concentrations of the cross-linking agent DSP. After washing with 8 M urea to remove un-cross-linked proteins, DSP-induced cross-links were reversed, and eluted proteins were analyzed by immunoblot analysis. Among the tail submodule subunits queried in this analysis, MED16 exhibited the most preferential cross-linking to GST-Neh4/5 (Fig. 2B), indicating that MED16 and NRF2 were in close proximity. In contrast, MED24 and MED23 exhibited less efficient cross-linking under the same conditions (Fig. 2B), suggesting that NRF2 does not directly target MED24 or MED23. Thus, we concluded that MED16 is the target subunit of NRF2 in the Mediator complex.

NRF2 interacts with N-terminal and intermediate regions of MED16. To map the regions of MED16 that interact with NRF2, we constructed expression vectors expressing truncated MED16 constructs with FLAG tags (Fig. 3A). The full-length MED16 protein was divided into four fragments, each of which was overexpressed in 293T cells. The whole-cell extract containing each MED16 fragment was mixed with GST-Neh4/5 or GST-Neh1, and GST pulldown assays were performed. Both the Neh4/5 and Neh1 domains were found to interact with the N-terminal region of MED16 (MED16-A), whereas a weak interaction was observed between the intermediate region of MED16 (MED16-C) and the Neh1 domain (Fig. 3B). These results indicate that the N-terminal region of MED16 contains a major NRF2-interacting domain, suggesting that MED16 is a direct interactant of NRF2.

***Med16* knockout cell lines exhibit normal proliferation.** The results described above implied that MED16 served as a key component of the Mediator complex for NRF2-mediated gene expression. To test this hypothesis, we disrupted the *Med16* gene in Hepa1c1c7 cells, which are derived from mouse hepatoma cells, by using the CRISPR/CAS9 system (27). To design the gRNA sequence for the *Med16* gene, we explored the domain architecture of MED16 by utilizing SMART (http://smart.embl-heidelberg.de). Two independent functional domains were predicted for MED16: a WD repeat-like domain and a MED16 conserved region, at amino acids 95 to 134 and 144 to 859, respectively, of the mouse MED16 protein (see Fig. S1 in the supplemental material). Based on this information, we chose a gRNA target sequence in exon III, encoding amino acids 82 to 117 of MED16, so that resultant truncated forms of MED16 would lose most of the functional domains (Fig. 4A).

We obtained 21 clones of *Med16*-disrupted Hepa1c1c7 cells (*Med16* KO cells), which exhibited no apparent changes in MED24 protein levels (Fig. 4B). Most of the clones appeared to proliferate at rates comparable to that of parental Hepa1c1c7 cells, except for a few slow growers. Two clones (*Med16* KO 1 and *Med16* KO 2) were arbitrarily selected from the healthy growers and examined for the *Med16* gene disruption. Genomic DNAs of *Med16* KO 1 and *Med16* KO 2 cells were PCR amplified with a primer set flanking the gRNA target site, and the amplicons were cloned and sequenced. Two deletion patterns were observed for each clone: 22-bp and 76-bp deletions in *Med16* KO 1 (see Fig. S2 in the supplemental material) and 1-bp and 36-bp deletions in *Med16* KO 2 (see Fig. S3). These results indicated that both *Med16* alleles were successfully disrupted at exon III in both *Med16* KO clones, resulting in the production of truncated forms of MED16 that contained, at best, only a partial WD repeat-like region. Thus, we used these *Med16* KO clones for further studies.

As an initial characterization of these *Med16* KO clones, we examined their proliferation rates and electrophile-responsive nuclear accumulation of NRF2. Proliferation rates of *Med16* KO 1 and *Med16* KO 2 cells were comparable to that of parental (WT) cells (Fig. 4C). Similarly, no significant difference was observed in the nuclear abundance of NRF2 after treatment with DEM, an NRF2-inducing electrophile, between WT and *Med16* KO cells (Fig. 4D).

MED16 depletion reduces the expression of NRF2 target genes. We next examined the functional contribution of MED16 to the NRF2-dependent stress response pathway. To globally investigate whether MED16 is required for NRF2-mediated tran-

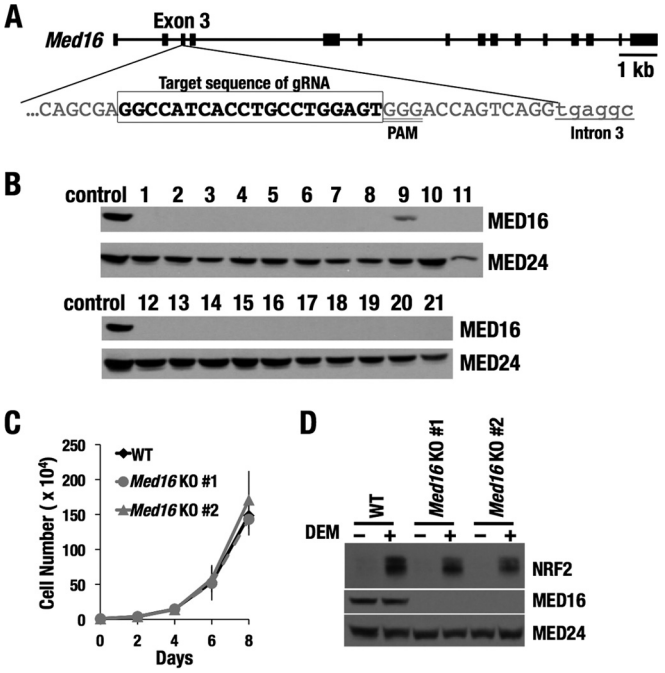

FIG 4 Establishment of MED16-depleted (*Med16* KO) Hepa1c1c7 cells. (A) Design of gRNA for the CRISPR/CAS9 system to disrupt the *Med16* gene. (B) Immunoblot analysis of 21 candidate clones of *Med16* KO cells in comparison with parental Hepa1c1c7 cells (control). MED16 and MED24 were detected. (C) Cell proliferation study of parental (WT) and *Med16* KO cells. (D) Immunoblot analysis of NRF2, MED16, and MED24 in WT and *Med16* KO cells treated with DEM or vehicle. Two independent clones of *Med16* KO cells (clones 1 and 2) were examined.

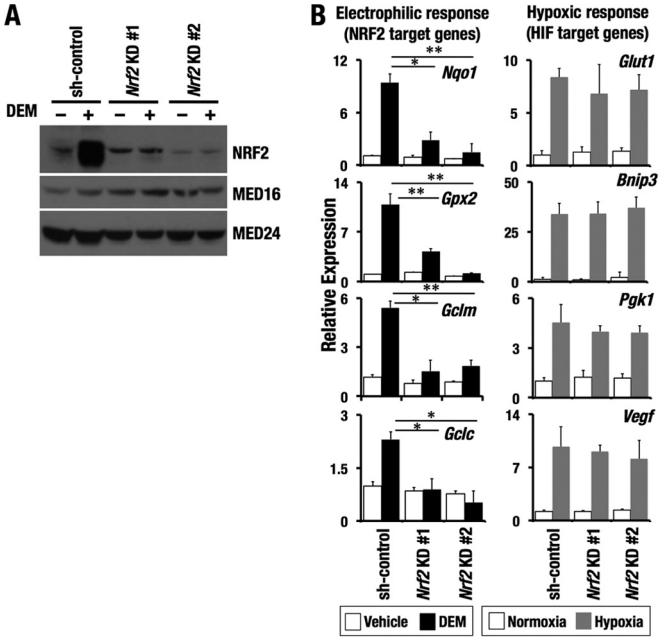

FIG 5 NRF2 deficiency sensitizes cells to oxidative stress. (A) Detection of NRF2, MED16, and MED24 by immunoblot analysis of control or *Nrf2* knockdown (*Nrf2* KD) Hepa1c1c7 cells treated with DEM or vehicle. (B) Relative expression levels of electrophile-responsive genes (left) and hypoxia-responsive genes (right) in Hepa1c1c7 cells treated with control or *Nrf2* shRNAs. Two different *Nrf2* shRNAs were used. *, $P < 0.01$; **, $P < 0.001$.

scriptional activation, we performed microarray analyses and compared the transcriptomes of *Med16* KO and WT Hepa1c1c7 cells treated with vehicle (DMSO) or DEM.

Among the genes activated by DEM in Hepa1c1c7 cells, NRF2-dependent genes that were activated in response to DEM needed to be selected. To this end, we generated *Nrf2* knockdown cells (*Nrf2* KD cells) by infecting Hepa1c1c7 cells with two different retroviral *Nrf2* shRNAs and confirmed that DEM-induced accumulation of NRF2 protein and elevation of its target genes were suppressed in *Nrf2* KD cells compared to control cells harboring control shRNA (sh-control cells) (Fig. 5A and B, left panels). MED16 and MED24 protein levels were comparable irrespective of *Nrf2* status (Fig. 5A). Expression levels of hypoxia-induced genes, which are targets of the hypoxia-inducible factor (HIF) transcription factors, were also not affected by *Nrf2* knockdown (Fig. 5B, right panels).

The transcriptomes of the *Nrf2* KD cells and sh-control cells treated with DEM or vehicle were examined by microarray analyses and compared with those of *Med16* KO and WT cells treated with DEM or vehicle. The genes comprising the intersection of the DEM-inducible gene sets in sh-control cells and WT cells were defined as the "DEM-activated genes." The DEM-activated genes were narrowed down to NRF2-dependent DEM-activated genes (NRF2-activated genes) if the DEM-induced fold change in *Nrf2* KD cells was smaller than that in sh-control cells (see Materials and Methods for details). Consequently, 848 genes were selected as NRF2-activated genes (see Table S1 in the supplemental material). The 848 genes were arranged in decreasing order of DEM-induced fold change differences between WT and *Med16* KO cells and divided into two groups, i.e., groups I and II (Fig. 6A). For the group I genes, DEM-induced transcriptional activation was blunted in the absence of MED16, whereas group II genes were either not affected by MED16 depletion or exhibited more induction in *Med16* KO cells than in WT cells. Amazingly, 639 of the 848 NRF2-activated genes (75%) fell into group I, in which most of the typical NRF2 target genes were included. A top hit signature of the group I genes from the Molecular Signatures Database (http://www.broadinstitute.org/gsea/msigdb/index.jsp) was xenobiotic metabolism, which is closely related to NRF2 function.

To verify the results of the microarray analyses, the expression levels of four representative NRF2 target genes were examined by RT-PCR. DEM-induced gene expression was significantly attenuated in *Med16* KO cells, whereas MED16 depletion had no effect on hypoxia-induced gene expression (Fig. 6B), which recapitulated the results obtained for *Nrf2* KD cells (Fig. 5B).

To rule out off-target effects of the gRNA used in the CRISPR/CAS9 system to disrupt *Med16*, we knocked down MED16 by use of siRNA in the human hepatoma cell line Hep3B (Fig. 7A). In good agreement with the results for *Med16* KO cells, *Med16* knockdown decreased the DEM-induced expression of NRF2 target genes in Hep3B cells but did not influence hypoxia-induced gene expression (Fig. 7B). Depletion of MED16 did not change the *NRF2* mRNA level (Fig. 7C). Therefore, these results indicate a specific requirement for MED16 in NRF2-dependent transcriptional activation.

The NRF2-interacting domain of MED16 is insufficient for inducible expression of NRF2 target genes. We next performed a rescue experiment for the MED16 loss-of-function phenotype to further rule out the off-target effects of the gRNA. To this end, we

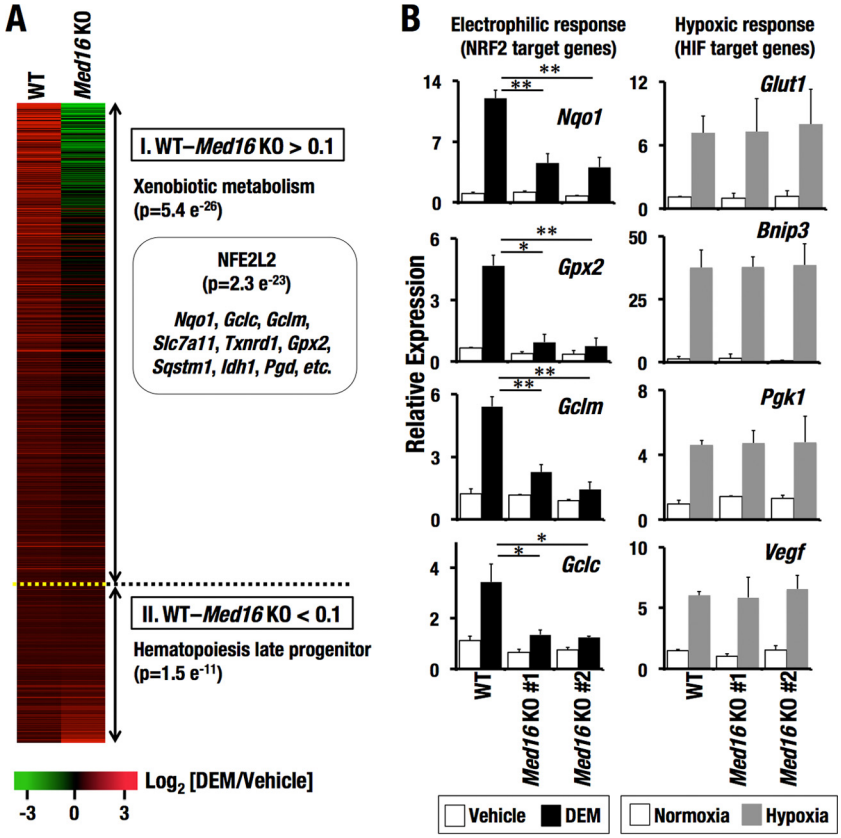

FIG 6 Depletion of MED16 mitigates the inducible expression of NRF2-activated genes in response to DEM. (A) Heat map showing DEM-induced fold changes for 848 NRF2-activated genes in control (WT) and *Med16* KO Hepa1c1c7 cells. The heat map colors represent the $\log_2$ fold changes in gene expression for DEM-treated cells versus vehicle-treated cells. The 848 NRF2-activated genes were aligned in decreasing order of the DEM-induced fold change difference between WT and *Med16* KO cells and divided into two groups, i.e., groups I and II. The overlap between the genes in each group and gene sets in the Molecular Signatures Database was investigated. The top hit signatures and their *P* values are shown. Typical NRF2 target genes are all included in group I. (B) Relative expression levels of electrophile-responsive genes (left) and hypoxia-responsive genes (right). Two independent clones of *Med16* KO cells (clones 1 and 2) were examined. *, $P < 0.01$; **, $P < 0.001$.

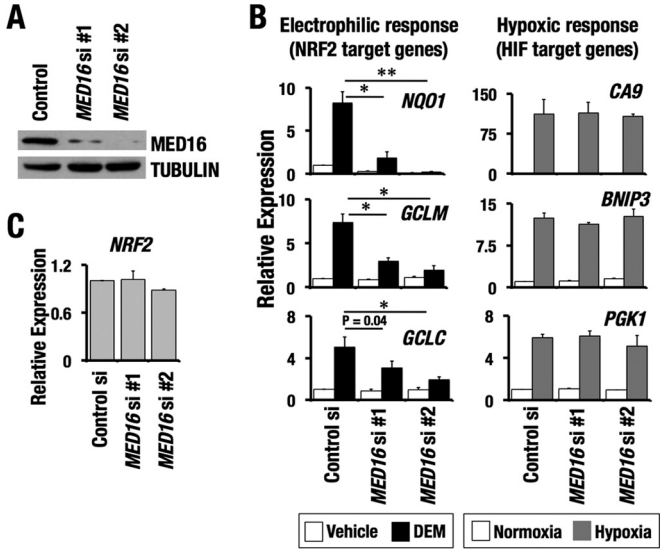

FIG 7 MED16 regulates NRF2 target gene expression in human hepatoma Hep3B cells. (A) Immunoblot analysis of MED16 expression in Hep3B cells treated with control or *MED16* siRNAs. (B) Relative expression levels of electrophile-responsive genes (left) and hypoxia-responsive genes (right) in Hep3B cells treated with control or *MED16* siRNAs. *, $P < 0.01$; **, $P < 0.001$. (C) Relative expression of *NRF2* in Hep3B cells treated with control or *MED16* siRNAs. Two different *MED16* siRNAs were used (siRNAs 1 and 2).

added the full-length human MED16 protein (FLAG-hMED16) back to the *Med16* KO cells (Fig. 8A). As expected, DEM-inducible expression of NRF2 target genes recovered nicely, to the levels in WT cells (Fig. 8B). Thus, we concluded that impaired induction of NRF2 target genes in *Med16* KO cells was specifically caused by the loss of function of MED16.

We applied this result to examine the activity of the N-terminal region of MED16, which contains the major NRF2-interacting domain (Fig. 3). We introduced an expression vector for the N-terminal region of MED16 (FLAG-hMED16-A) into *Med16* KO cells (Fig. 8A). Importantly, MED16-A failed to rescue the impaired induction of NRF2 target genes (Fig. 8B), despite the fact that the MED16-A expression level was much higher than that of full-length MED16 (Fig. 8A). This result suggests that the N-terminal region of MED16 does not mediate NRF2-dependent transcriptional activation. It should be noted that whereas full-length MED16 interacted with MED24, MED16-A did not interact with MED24 (Fig. 8C), suggesting that the C-terminal region of MED16 is required for its association with the Mediator complex, possibly through the submodule components, including MED24. Therefore, to achieve electrophile-inducible transcriptional activation, MED16 bridges the interaction between NRF2 and the Mediator complex by binding to the former and the latter by using its N-terminal and C-terminal regions, respectively.

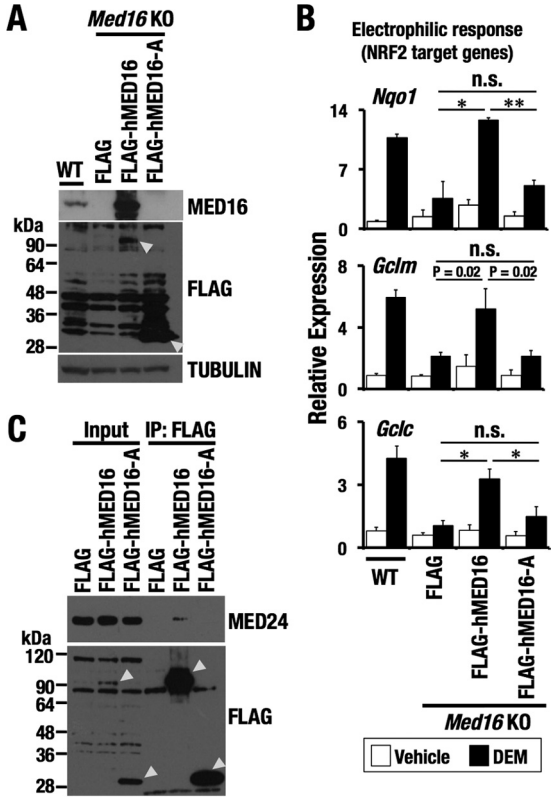

FIG 8 Truncated MED16 missing the domain for interaction with MED24 does not support the DEM-inducible expression of NRF2 target genes. (A) Immunoblot analysis of FLAG-tagged full-length MED16 and an N-terminal fragment of MED16 (MED16-A) expressed in *Med16* KO Hela1c1c7 cells. (B) Relative expression levels of electrophile-responsive genes in WT cells and *Med16* KO cells expressing FLAG, FLAG-MED16, or FLAG-MED16-A. *, $P < 0.01$; **, $P < 0.001$; n.s., not significant. (C) Immunoprecipitation assay of whole-cell extracts prepared from *Med16* KO cells expressing FLAG, FLAG-MED16, or FLAG-MED16-A. *Med16* KO 1 cells were used.

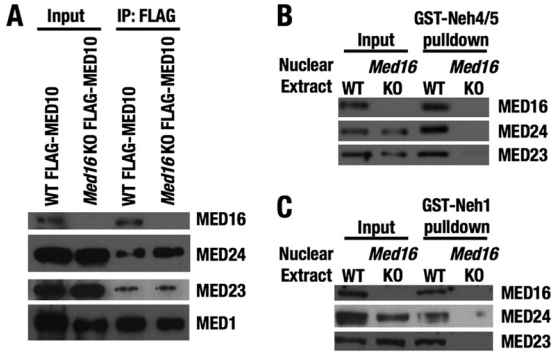

FIG 9 MED16 is required for the association of MED23 and MED24 with NRF2. (A) Comparison of the Mediator complex in WT and *Med16* KO Hepa1c1c7 cells. FLAG-MED10-expressing WT and *Med16* KO cells were established. MED16, MED24, and MED23 were detected as components of the submodule, and MED1 was detected as a representative subunit of the main body of the Mediator complex. (B and C) GST-NRF2 pulldown assays with nuclear extracts from WT or *Med16* KO cells. GST-Neh4/5 (B) and GST-Neh1 (C) were used for the pulldown assays. *Med16* KO 1 cells were used.

MED16 is required for tethering of the Mediator complex to NRF2. It has been reported that MED16 forms a tight submodule with MED24 and MED23 in the tail module of the Mediator complex and that loss of either MED24 or MED23 results in reduction of the whole submodule in the Mediator complex (25, 26). According to these reports, we suspected that the MED16-deficient Mediator complex may lack MED24 and MED23. To characterize the Mediator complex in *Med16* KO cells, we stably introduced the FLAG-MED10 expression vector into WT and *Med16* KO Hepa1c1c7 cells and isolated the Mediator complex from the FLAG-MED10-expressing cells with or without MED16 by using the anti-FLAG antibody. The Mediator complex from *Med16* KO cells contained levels of MED24, MED23, and MED1 similar to those in WT cells (Fig. 9A), suggesting that the Mediator complex is intact in *Med16* KO cells, except for the absence of MED16. These results also suggest that MED16 may be dispensable for the integrity of the whole Mediator complex.

We then addressed the central question of whether MED16 is required for the interaction of the Mediator complex with NRF2. For this purpose, nuclear extracts from WT and *Med16* KO cells were incubated with GST-Neh4/5. GST pulldown assay revealed that depletion of MED16 remarkably reduced the interaction of GST-Neh4/5 with MED24 and MED23 (Fig. 9B). A similar result was obtained for the interaction of GST-Neh1 (Fig. 9C). Since MED24 and MED23 were present in the Mediator complex in *Med16* KO cells (Fig. 9A), the absence of MED24 and MED23 in the NRF2 interactants indicated that the Mediator complex was not recruited to NRF2 in *Med16* KO cells. Therefore, MED16 tethers the Mediator complex to the Neh4/5 and Neh1 domains of NRF2 independently of the other submodule members, MED24 and MED23.

Endogenous MED16 associates with NRF2 and is recruited to the NRF2 target gene loci. To confirm an endogenous interaction between MED16 and NRF2, we performed an immunoprecipitation assay using liver protein extracts prepared from liver-specific double-mutant mice with mutations of the *Pten* and *Keap1* genes (*Pten*$^{flox/flox}$::*Keap1*$^{flox/flox}$::*Albumin*-Cre mice [PK-Alb mice]). PK-Alb mice were used for the immunoprecipitation assay because nuclear accumulation of NRF2 is greatly enhanced in these mice due to the simultaneous inhibition of two independent degradation pathways of NRF2, i.e., the Keap1-Cul3-dependent and β-TrCP-Cul1-dependent degradation pathways (28, 29). Endogenous NRF2 and its interactants were immunoprecipitated with anti-NRF2 antibody. The Mediator subunits MED16, MED23, MED24, MED14, and MED1 were copurified as unique interactants of NRF2, concomitant with CBP and p300, in two independent gel-based LC-MS/MS analyses (Fig. 10A). Endogenous associations of NRF2 with MED16 and MED24 were confirmed in the immunoblot analyses as well (Fig. 10B).

We then performed a ChIP assay to examine the recruitment of endogenous MED16 to the NRF2 target genes. Because available anti-MED16 antibodies worked for human MED16 but not for mouse MED16 in the ChIP assay, we used the human lung adenocarcinoma cell line A549, in which NRF2 is constitutively stabilized due to *KEAP1* mutation. NRF2-dependent recruitment of MED16 was examined by comparing A549 cells with and without *NRF2* knockdown. NRF2 binding to the AREs of both the *NQO1* and *GCLM* genes, which are typical NRF2 target genes, was dramatically reduced after *NRF2* knockdown in three independent experiments (Fig. 10C, lower panels). The interaction of MED16 with these AREs was similarly reduced by *NRF2* knockdown (Fig. 10C, upper panels), demonstrating the NRF2-dependent recruitment of endogenous MED16 to the NRF2 target sites.

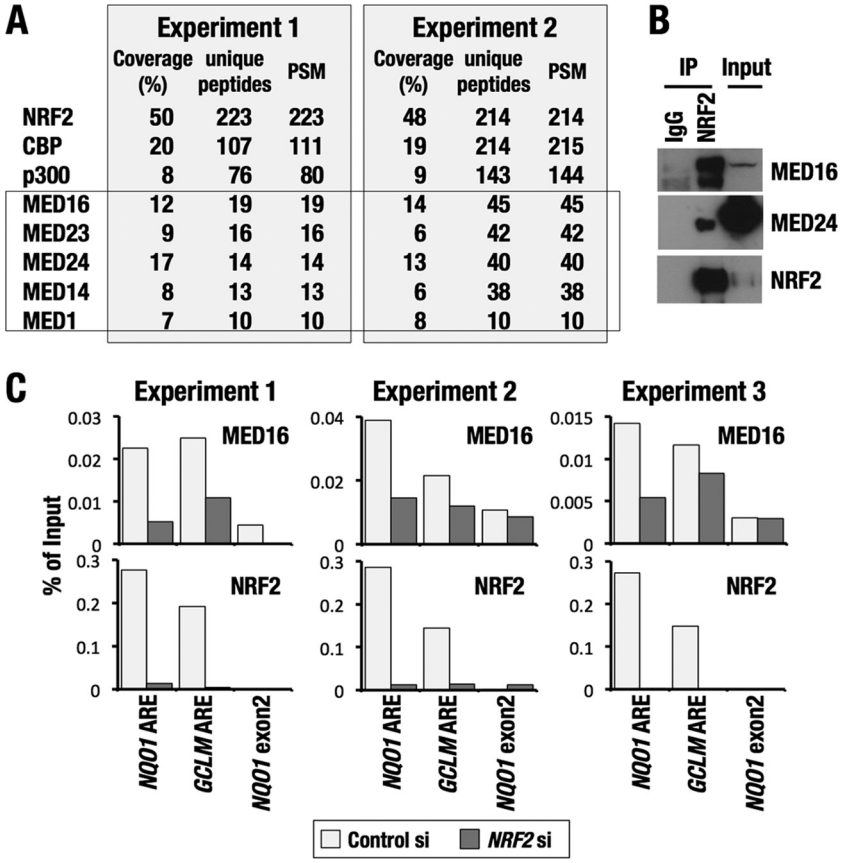

FIG 10 Endogenous interaction between MED16 and NRF2. (A) List of NRF2-interacting proteins from PK-Alb mouse liver as identified by LC-MS/MS. PSM, total peptide spectrum matches. (B) Immunoblot analysis of Mediator subunits and NRF2 in the endogenous NRF2 complex purified from PK-Alb mouse liver. (C) Quantitative ChIP assays of MED16 and NRF2 at the NRF2 binding sites (*NQO1* ARE and *GCLM* ARE) and negative locus (*NQO1* exon 2) in A549 cells with or without NRF2 knockdown. Results of three independent experiments are shown.

MED16 is required for NRF2-dependent phosphorylation of the RNAP II C-terminal domain. Because MED16 depletion did not reduce the nuclear accumulation of NRF2 (Fig. 4D) yet decreased the expression of NRF2 target genes (Fig. 6 and 7) in response to DEM, we surmised that MED16 contributes to the recruitment and/or activation of RNAP II by tethering the Mediator complex to NRF2.

To test this hypothesis, we performed a ChIP analysis using WT and *Med16* KO cells. The ChIP assay showed that DEM-induced recruitment of NRF2 to the ARE was comparable between WT and *Med16* KO cells (Fig. 11A and B, left panels), indicating that MED16 does not influence the availability of NRF2 at AREs. CBP recruitment to the ARE was enhanced by DEM treatment, consistent with the current notion that CBP binds to NRF2 as a coactivator (11), and this binding was also unaffected by the MED16 deficiency (Fig. 11A and B, right panels).

Next, we examined RNAP II recruitment to NRF2 target gene loci (Fig. 11A and C, left panels). In WT cells, DEM treatment increased RNAP II recruitment to the *Nqo1* transcription start site (TSS), but the increase was not apparent for the *Gclm* and *Gclc* TSSs, suggesting that *Nqo1* exhibits NRF2-dependent RNAP II recruitment. *Med16* KO cells gave almost the same results, indicating that MED16 does not play a major role in NRF2-dependent RNAP II recruitment.

We then examined the phosphorylation status of the C-terminal domain (CTD) of RPB1, the largest subunit of RNAP II. Ser5 and Ser2 phosphorylations (S5P and S2P, respectively) of the CTD were examined in NRF2 target gene loci (Fig. 11A and C, right and middle panels). In WT cells, the S5P-CTD level at the *Nqo1* TSS and the S2P-CTD levels at the downstream regions of *Nqo1*, *Gclm*, and *Gclc* were elevated concomitantly with the DEM-induced recruitment of NRF2. These elevations were all absent in *Med16* KO cells, suggesting that MED16 depletion abrogates the NRF2-dependent increase of RNAP II CTD phosphorylation, which further suggests a collaborative function of NRF2 and MED16 in the regulation of RNAP II activation.

MED16 is required for NRF2-dependent cellular protection against oxidative stress. Finally, we tested whether the depletion of MED16 sensitized Hepa1c1c7 cells to oxidative insults. The *Nrf2* knockdown Hepa1c1c7 cells were dramatically vulnerable to cytotoxicity induced by menadione, an oxidative stress-inducing chemical (Fig. 12A). Increasing concentrations of menadione were applied to WT and *Med16* KO cells. As expected, *Med16* KO cells were susceptible to oxidative insults similarly to *Nrf2* knockdown cells (Fig. 12B). From these results, we conclude that MED16 transmits electrophilic signals sensed by the KEAP1-NRF2 system to RNAP II to activate cytoprotective genes, achieving the antioxidant response.

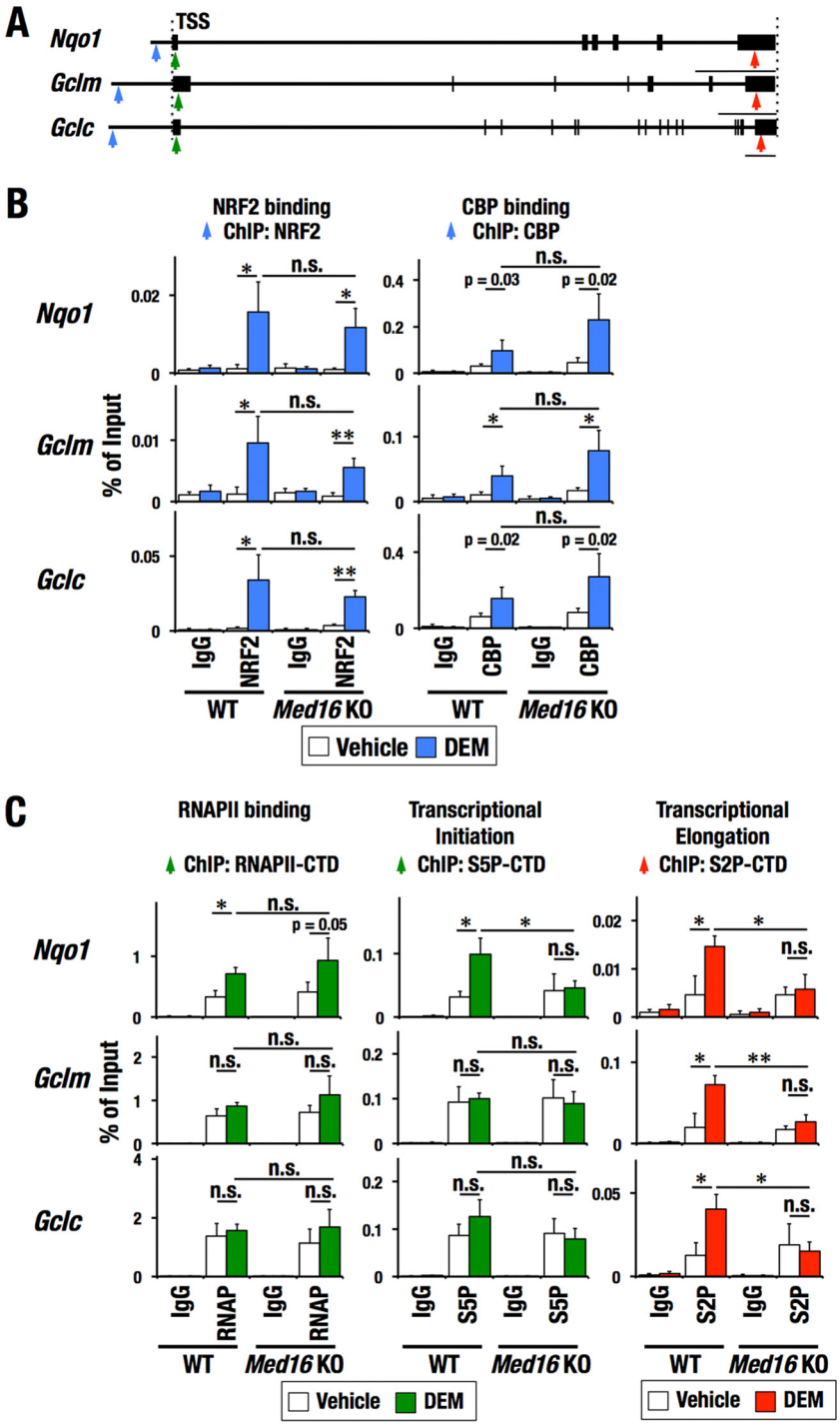

FIG 11 MED16 regulates RNAP II CTD phosphorylation without affecting NRF2 binding to the ARE. (A) Positions of primer sets used for ChIP assay within each target gene locus (*Nqo1*, *Gclm*, and *Gclc*). TSS, transcription start site. Blue, green, and red arrows indicate the positions of primer sets for examining NRF2 binding to the ARE, S5P-CTD levels around the TSS, and S2P-CTD levels at the downstream region of each gene, respectively. Scale bars indicate 2 kbp. (B and C) Quantitative ChIP assay at each target gene locus in WT and *Med16* KO Hepa1c1c7 cells. Localization of NRF2 and CBP (B) and of RNAP-CTD, S5P-CTD, and S2P-CTD (C) was examined in WT and *Med16* KO cells treated with DEM or vehicle. *Med16* KO 1 cells were used. Error bars show standard deviations. *, $P < 0.05$; **, $P < 0.01$; n.s., not significant.

DISCUSSION

In this study, we identified MED16 as a specific cofactor that bridges NRF2 and the Mediator complex for the inducible expression of a majority of the NRF2 target genes. Once toxic chemicals in the environment (often electrophilic signals) are sensed by KEAP1 in the cytoplasm, NRF2 is stabilized and accumulates in the nucleus. Therefore, the signals transmitted to NRF2 are conveyed to the nucleus and transduced to the robust transcriptional

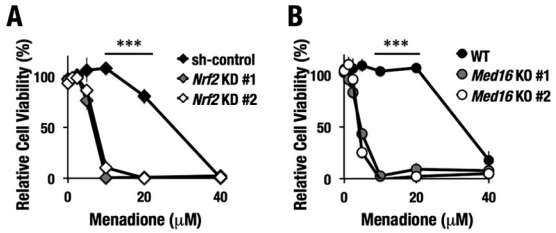

FIG 12 Depletion of NRF2 or MED16 results in vulnerability to oxidative stress. (A) Relative viabilities of WT and *Nrf2* knockdown Hepa1c1c7 cells after 24 h of treatment with menadione. Two different *Nrf2* shRNAs (1 and 2) were used. (B) Relative viabilities of WT and *Med16* KO Hepa1c1c7 cells after 24 h of treatment with menadione. Two independent clones of *Med16* KO cells (1 and 2) were examined. Error bars show standard deviations. ***, $P < 1 \times 10^{-4}$.

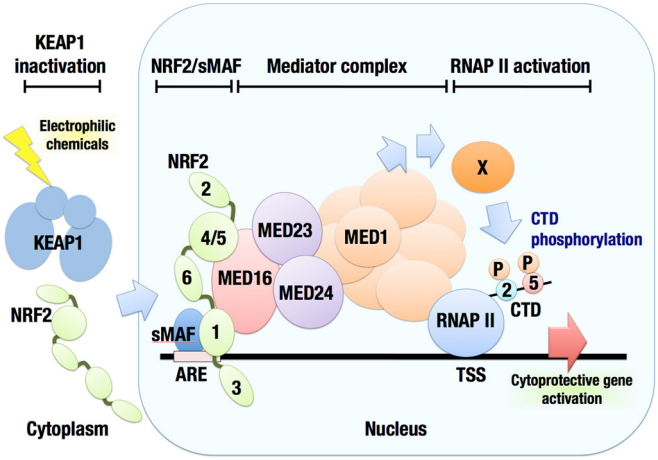

FIG 13 Illustration of the KEAP1-NRF2-MED16 axis for the antioxidant response. MED16 serves as a conduit of the Mediator complex, transmitting electrophilic signals from NRF2 to RNAP II. A model deduced from the results of this study is shown in a rounded square indicating a nucleus. Numbers 1 to 6 marked in NRF2 indicate the domain names corresponding to Neh1 to Neh6.

activation of cytoprotective enzyme genes. However, the molecular mechanisms supporting the powerful transactivation by NRF2 have not been elucidated in detail. This study has clarified that the Mediator complex is one of the critical coactivator components conferring a potent transcription activation ability on NRF2, concomitant with the CBP/p300 histone acetyltransferase. As illustrated in Fig. 13, this study provides solid evidence for the first time that MED16 is an efficient NRF2-interacting interface of the Mediator complex, which transmits environmental stress signals to the basal transcription machinery for the final output. Thus, our discovery of MED16 as a conduit for NRF2 has provided the missing intranuclear piece of the KEAP1-NRF2 pathway and revealed the KEAP1-NRF2-MED16 axis as a major antioxidant mechanism.

In addition to the Mediator subunits, we obtained CBP and p300 in the NRF2 nuclear protein complex, which is in good agreement with our previous results (11). Indeed, we observed that NRF2 and CBP are both recruited to AREs after DEM treatment. Histone-modifying enzymes, such as CBP/p300, are recruited first to the promoter upon DNA binding of a signal-specific transcription factor, and they make the chromatin structure permissive for transcription. Subsequently, Mediator is recruited and directs the assembly of the preinitiation complex (PIC) (30, 31). Consistent with the notion that CBP is recruited to AREs prior to the Mediator complex, our ChIP assay demonstrated that MED16 deficiency and resultant defective tethering of the Mediator complex do not affect the recruitment of CBP to AREs.

In contrast, MED16 deficiency suppresses the NRF2-dependent phosphorylation of the RNAP II CTD, whereas RNAP II recruitment levels are similar irrespective of the MED16 status. The S5P-CTD and S2P-CTD constructs examined in this study characterized RNAP II at the initiation phase and the elongation phase, respectively (32, 33). At the *Nqo1* TSS, RNAP II is recruited concomitantly with NRF2, and phosphorylations of both S5P-CTD and S2P-CTD are increased in a MED16-dependent manner, suggesting that NRF2 and MED16 cooperatively promote transcription initiation at the *Nqo1* gene. In contrast, at the *Gclc* and *Gclm* TSSs, S5P-CTD levels are constant before and after DEM-induced NRF2 recruitment, implying that an NRF2-independent mechanism may exist for transcription initiation at these gene loci. Interestingly, S2P-CTD levels at *Gclc* and *Gclm* loci are increased when NRF2 is activated by DEM, in a MED16-dependent manner, suggesting that NRF2 and MED16 may make substantial contributions to transcriptional elongation for these genes. Thus, the NRF2-MED16 combination contributes to RNAP II activation, although the precise mechanisms seem to differ depending on the genomic context.

MED16 is a component of a tight submodule with MED24 and MED23 in the tail module of the Mediator complex. One of the salient findings of the present study is that MED16 can be depleted without affecting MED24 and MED23 in the Mediator complex. In contrast, loss of MED24 and MED23 results in the disassembly of the remaining submodule from the Mediator complex. A connotation here is that MED16 is positioned at the tip of the submodule and binds to NRF2 for tethering of the whole Mediator complex. Note that MED16 binds to NRF2 and MED24 (possibly linking to the rest of the Mediator complex) by using its N-terminal and C-terminal regions, respectively, and that both interactions are essential for NRF2-dependent transcriptional activation.

Each subunit of the submodule appears to serve as an independent conduit for a distinct signaling pathway. For instance, in *Drosophila*, MED23 enhances the heat shock-induced gene expression mediated by heat shock factor (HSF), whereas MED16 is responsible for the lipopolysaccharide (LPS)-induced gene expression mediated by dorsal-related immunity factor (DIF), an NF-κB ortholog (34). In any case, the tail submodule provides an interface between Mediator and signal-specific transcription factors, especially those responding to environmental stresses. NRF2, NF-κB, and HSF respond to electrophilic chemicals, inflammation, and heat shock, respectively.

In contrast, HIF is responsible for the hypoxic response and does not require MED16, suggesting that an alternative Mediator interface receives the hypoxic signal. Indeed, HIF1α associates directly with CDK8, MED12, and MED13, which comprise the kinase module of the Mediator (35), indicating that hypoxic signals are channeled through the kinase module. Among the components of the kinase module, MED12 interacts with aryl hydrocarbon receptor nuclear translocator (ARNT), a heterodimeric partner shared by HIF1α and the aryl hydrocarbon receptor (AHR) that is indispensable for the AHR-dependent xenobiotic response as well as the HIF-dependent hypoxic response (36).

Thus, environmental stress-responsive transcription factors utilize specific subunits of Mediator, primarily those in the tail and kinase modules, to achieve transcriptional activation of their target genes. Our study has clarified the overall picture of transcriptional activation in the environmental stress response by drawing an additional line connecting electrophilic chemicals and MED16 via NRF2.

ACKNOWLEDGMENTS

We thank Keiko Taguchi for providing experimental materials, Masanobu Morita for advice on the CRISPR/CAS9 system, Koichiro Kato and Tatsuro Iso for technical support for recombinant protein preparation, Kyoko Ochiai for advice on protein purification, and the Biomedical Research Core of the Tohoku University Graduate School of Medicine for technical support.

We have no competing interests to declare.

H. Sekine designed the study, conducted the experiments, analyzed the data, and wrote early drafts of the paper. K. Okazaki, N. Ota, H. Shima, and Y. Katoh conducted the experiments and analyzed the data. N. Suzuki, K. Igarashi, and M. Ito contributed to the data analysis. H. Motohashi supervised the research, analyzed the data, and wrote early drafts of the paper. M. Yamamoto supervised the research and wrote the manuscript.

FUNDING INFORMATION

Ministry of Education, Culture, Sports, Science, and Technology (MEXT) provided funding to Hozumi Motohashi under grant number 23116002. Ministry of Education, Culture, Sports, Science, and Technology (MEXT) provided funding to Norio Suzuki under grant number 26116702. Ministry of Education, Culture, Sports, Science, and Technology (MEXT) provided funding to Masayuki Yamamoto and Norio Suzuki under grant number 26111002. Japan Society for the Promotion of Science (JSPS) provided funding to Masayuki Yamamoto under grant number 24249015. Japan Society for the Promotion of Science (JSPS) provided funding to Hozumi Motohashi under grant numbers 24390075, 15H-4692, and 26670150. Core Research for Evolutional Science and Technology, Japan Science and Technology Agency (CREST, JST) provided funding to Hozumi Motohashi and Masayuki Yamamoto. Daiichi Sankyo Foundation of Life Science provided funding to Hozumi Motohashi. Uehara Memorial Foundation provided funding to Hozumi Motohashi.

The funders had no role in study design, data collection and interpretation, or the decision to submit the work for publication.

REFERENCES

1. **Motohashi H, Yamamoto M.** 2004. Nrf2-Keap1 defines a physiologically important stress response mechanism. Trends Mol Med **10:**549–557. http://dx.doi.org/10.1016/j.molmed.2004.09.003.
2. **Uruno A, Motohashi H.** 2011. The Keap1-Nrf2 system as an in vivo sensor for electrophiles. Nitric Oxide **25:**153–160. http://dx.doi.org/10.1016/j.niox.2011.02.007.
3. **Malhotra D, Portales-Casamar E, Singh A, Srivastava S, Arenillas D, Happel C, Shyr C, Wakabayashi N, Kensler TW, Wasserman WW, Biswal S.** 2010. Global mapping of binding sites for Nrf2 identifies novel targets in cell survival response through ChIP-Seq profiling and network analysis. Nucleic Acids Res **38:**5718–5734. http://dx.doi.org/10.1093/nar/gkq212.
4. **Chorley BN, Campbell MR, Wang X, Karaca M, Sambandan D, Bangura F, Xue P, Pi J, Kleeberger SR, Bell DA.** 2012. Identification of novel NRF2-regulated genes by ChIP-Seq: influence on retinoid X receptor alpha. Nucleic Acids Res **40:**7416–7429. http://dx.doi.org/10.1093/nar/gks409.
5. **Hirotsu Y, Katsuoka F, Funayama R, Nagashima T, Nishida Y, Nakayama K, Engel JD, Yamamoto M.** 2012. Nrf2-MafG heterodimers contribute globally to antioxidant and metabolic networks. Nucleic Acids Res **40:**10228–10239. http://dx.doi.org/10.1093/nar/gks827.
6. **Malik S, Roeder RG.** 2010. The metazoan Mediator co-activator complex as an integrative hub for transcriptional regulation. Nat Rev Genet **11:**761–772. http://dx.doi.org/10.1038/nrg2901.
7. **Allen BL, Taatjes DJ.** 2015. The Mediator complex: a central integrator of transcription. Nat Rev Mol Cell Biol **16:**155–166. http://dx.doi.org/10.1038/nrm3951.
8. **Itoh K, Wakabayashi N, Katoh Y, Ishii T, Igarashi K, Engel JD, Yamamoto M.** 1999. Keap1 represses nuclear activation of antioxidant responsive elements by Nrf2 through binding to the amino-terminal Neh2 domain. Genes Dev **13:**76–86. http://dx.doi.org/10.1101/gad.13.1.76.
9. **Katoh Y, Iida K, Kang MI, Kobayashi A, Mizukami M, Tong KI, McMahon M, Hayes JD, Itoh K, Yamamoto M.** 2005. Evolutionary conserved N-terminal domain of Nrf2 is essential for the Keap1-mediated degradation of the protein by proteasome. Arch Biochem Biophys **433:**342–350. http://dx.doi.org/10.1016/j.abb.2004.10.012.
10. **Chowdhry S, Zhang Y, McMahon M, Sutherland C, Cuadrado A, Hayes JD.** 2013. Nrf2 is controlled by two distinct β-TrCP recognition motifs in its Neh6 domain, one of which can be modulated by GSK-3 activity. Oncogene **32:**3765–3781. http://dx.doi.org/10.1038/onc.2012.388.
11. **Katoh Y, Itoh K, Yoshida E, Miyagishi M, Fukamizu A, Yamamoto M.** 2001. Two domains of Nrf2 cooperatively bind CBP, a CREB binding protein, and synergistically activate transcription. Genes Cells **6:**857–868. http://dx.doi.org/10.1046/j.1365-2443.2001.00469.x.
12. **Zhang J, Hosoya T, Maruyama A, Nishikawa K, Maher JM, Ohta T, Motohashi H, Fukamizu A, Shibahara S, Itoh K, Yamamoto M.** 2007. Nrf2 Neh5 domain is differentially utilized in the transactivation of cytoprotective genes. Biochem J **404:**459–466. http://dx.doi.org/10.1042/BJ20061611.
13. **Nioi P, Nguyen T, Sherratt PJ, Pickett CB.** 2005. The carboxy-terminal Neh3 domain of Nrf2 is required for transcriptional activation. Mol Cell Biol **25:**10895–10906. http://dx.doi.org/10.1128/MCB.25.24.10895-10906.2005.
14. **Horie Y, Suzuki A, Kataoka E, Sasaki T, Hamada K, Sasaki J, Mizuno K, Hasegawa G, Kishimoto H, Iizuka M, Naito M, Enomoto K, Watanabe S, Mak TW, Nakano T.** 2004. Hepatocyte-specific Pten deficiency results in steatohepatitis and hepatocellular carcinomas. J Clin Invest **113:**1774–1783. http://dx.doi.org/10.1172/JCI20513.
15. **Okawa H, Motohashi H, Kobayashi A, Aburatani H, Kensler TW, Yamamoto M.** 2006. Hepatocyte-specific deletion of the keap1 gene activates Nrf2 and confers potent resistance against acute drug toxicity. Biochem Biophys Res Commun **339:**79–88. http://dx.doi.org/10.1016/j.bbrc.2005.10.185.
16. **Postic C, Magnuson MA.** 2000. DNA excision in liver by an albumin-Cre transgene occurs progressively with age. Genesis **26:**149–150. http://dx.doi.org/10.1002/(SICI)1526-968X(200002)26:2<149::AID-GENE16>3.0.CO;2-V.
17. **Sekine H, Mimura J, Oshima M, Okawa H, Kanno J, Igarashi K, Gonzalez FJ, Ikuta T, Kawajiri K, Fujii-Kuriyama Y.** 2009. Hypersensitivity of aryl hydrocarbon receptor-deficient mice to lipopolysaccharide-induced septic shock. Mol Cell Biol **29:**6391–6400. http://dx.doi.org/10.1128/MCB.00337-09.
18. **Maruyama A, Tsukamoto S, Nishikawa K, Yoshida A, Harada N, Motojima K, Ishii T, Nakane A, Yamamoto M, Itoh K.** 2008. Nrf2 regulates the alternative first exons of CD36 in macrophages through specific antioxidant response elements. Arch Biochem Biophys **477:**139–145. http://dx.doi.org/10.1016/j.abb.2008.06.004.
19. **Malik S, Roeder RG.** 2003. Isolation and functional characterization of the TRAP/mediator complex. Methods Enzymol **364:**257–284. http://dx.doi.org/10.1016/S0076-6879(03)64015-2.
20. **Kim S, Xu X, Hecht A, Boyer TG.** 2006. Mediator is a transducer of Wnt/beta-catenin signaling. J Biol Chem **281:**14066–14075. http://dx.doi.org/10.1074/jbc.M602696200.
21. **Lawrence AM, Besir HU.** 2009. Staining of proteins in gels with Coomassie G-250 without organic solvent and acetic acid. J Vis Exp **30:**e1350. http://dx.doi.org/10.3791/1350.
22. **Kalli A, Smith GT, Sweredoski MJ, Hess S.** 2013. Evaluation and optimization of mass spectrometric settings during data-dependent acquisition mode: focus on LTQ-Orbitrap mass analyzers. J Proteome Res **12:**3071–3086. http://dx.doi.org/10.1021/pr3011588.
23. **Stasevich TJ, Hayashi-Takanaka Y, Sato Y, Maehara K, Ohkawa Y, Sakata-Sogawa K, Tokunaga M, Nagase T, Nozaki N, McNally JG, Kimura H.** 2014. Regulation of RNA polymerase II activation by histone acetylation in single living cells. Nature **516:**272–275. http://dx.doi.org/10.1038/nature13714.
24. **Shibata T, Ohta T, Tong KI, Kokubu A, Odogawa R, Tsuta K, Asamura**

H, Yamamoto M, Hirohashi S. 2008. Cancer related mutations in NRF2 impair its recognition by Keap1-Cul3 E3 ligase and promote malignancy. Proc Natl Acad Sci U S A **105:**13568–13573. http://dx.doi.org/10.1073/pnas.0806268105.

25. **Ito M, Okano HJ, Darnell RB, Roeder RG.** 2002. The TRAP100 component of the TRAP/Mediator complex is essential in broad transcriptional events and development. EMBO J **21:**3464–3475. http://dx.doi.org/10.1093/emboj/cdf348.
26. **Stevens JL, Cantin GT, Wang G, Shevchenko A, Berk AJ.** 2002. Transcription control by E1A and MAP kinase pathway via Sur2 mediator subunit. Science **296:**755–758. http://dx.doi.org/10.1126/science.1068943.
27. **Yang H, Wang H, Shivalila CS, Cheng AW, Shi L, Jaenisch R.** 2013. One-step generation of mice carrying reporter and conditional alleles by CRISPR/Cas-mediated genome engineering. Cell **154:**1370–1379. http://dx.doi.org/10.1016/j.cell.2013.08.022.
28. **Mitsuishi Y, Taguchi K, Kawatani Y, Shibata T, Nukiwa T, Aburatani H, Yamamoto M, Motohashi H.** 2012. Nrf2 redirects glucose and glutamine into anabolic pathways in metabolic reprogramming. Cancer Cell **22:**66–79. http://dx.doi.org/10.1016/j.ccr.2012.05.016.
29. **Taguchi K, Hirano I, Itoh T, Tanaka M, Miyajima A, Suzuki A, Motohashi H, Yamamoto M.** 2014. Nrf2 enhances cholangiocyte expansion in Pten-deficient livers. Mol Cell Biol **34:**900–913. http://dx.doi.org/10.1128/MCB.01384-13.
30. **Métivier R, Penot G, Hübner MR, Reid G, Brand H, Kos M, Gannon F.** 2003. Estrogen receptor-alpha directs ordered, cyclical, and combinatorial recruitment of cofactors on a natural target promoter. Cell **115:**751–763. http://dx.doi.org/10.1016/S0092-8674(03)00934-6.
31. **Sharma D, Fondell JD.** 2002. Ordered recruitment of histone acetyltransferases and the TRAP/Mediator complex to thyroid hormone-responsive promoters in vivo. Proc Natl Acad Sci U S A **99:**7934–7939. http://dx.doi.org/10.1073/pnas.122004799.
32. **Buratowski S.** 2009. Progression through the RNA polymerase II CTD cycle. Mol Cell **36:**541–546. http://dx.doi.org/10.1016/j.molcel.2009.10.019.
33. **Egloff S, Dienstbier M, Murphy S.** 2012. Updating the RNA polymerase CTD code: adding gene-specific layers. Trends Genet **28:**333–341. http://dx.doi.org/10.1016/j.tig.2012.03.007.
34. **Kim TW, Kwon YJ, Kim JM, Song YH, Kim SN, Kim YJ.** 2004. MED16 and MED23 of Mediator are coactivators of lipopolysaccharide- and heat-shock-induced transcriptional activators. Proc Natl Acad Sci U S A **101:**12153–12158. http://dx.doi.org/10.1073/pnas.0401985101.
35. **Galbraith MD, Allen MA, Bensard CL, Wang X, Schwinn MK, Qin B, Long HW, Daniels DL, Hahn WC, Dowell RD, Espinosa JM.** 2013. HIF1A employs CDK8-mediator to stimulate RNAPII elongation in response to hypoxia. Cell **153:**1327–1339. http://dx.doi.org/10.1016/j.cell.2013.04.048.
36. **Beischlag TV, Taylor RT, Rose DW, Yoon D, Chen Y, Lee WH, Rosenfeld MG, Hankinson O.** 2004. Recruitment of thyroid hormone receptor/retinoblastoma-interacting protein 230 by the aryl hydrocarbon receptor nuclear translocator is required for the transcriptional response to both dioxin and hypoxia. J Biol Chem **279:**54620–54628. http://dx.doi.org/10.1074/jbc.M410456200.
37. **Ando R, Shima H, Tamahara T, Sato Y, Watabane-Matsui M, Kato H, Sax N, Motohashi H, Taguchi K, Yamamoto M, Nio M, Maeda T, Ochiai K, Muto A, Igarashi K.** The transcription factor Bach2 is phosphorylated at mutiple sites in murine B cells but a single site prevents its nuclear localization. J Biol Chem, in press. http://dx.doi.org/10.1074/jbc.M115.661702.